INTERNAL FRICTION STUDY OF THE HIGH TEMPERATURE DISLOCATION MOBILITY IN Si SINGLE CRYSTALS

P. Gadaud, J. Woirgard, P. Mazot, J. Demenet, J. de Fouquet

JOURNAL DE PHYSIQUE
Colloque C8, supplément au n°12, Tome 48, décembre 1987

INTERNAL FRICTION STUDY OF THE HIGH TEMPERATURE DISLOCATION MOBILITY IN Si SINGLE CRYSTALS

P. GADAUD, J. WOIRGARD, P. MAZOT, J.L. DEMENET* and J. de FOUQUET

Laboratoire de Mécanique et de Physique des Matériaux, ENSMA, Rue Guillaume VII, F-86034 Poitiers Cedex, France
**Laboratoire de Métallurgie Physique, Faculté des Sciences, Av. du Recteur Pineau, F-86000 Poitiers, France*

Abstract
Dislocation mobility in Silicon single crystals was studied by isothermal internal friction measurements. In prestrained single crystals three relaxation peaks, superimposed onto a low frequency background, were observed.
The first peak corresponds to the migration of geometrical kinks which leads to a rather high migration energy W_m of 1.5 eV. The second one corresponds to a complex mechanism involving nucleation and migration of interacting kinks on straight dislocation segments. From the measured activation energy (W_m + 1/2 F_{DK} = 1.95 eV), we obtain a kink formation energy of 0.9 eV, lower than the migration energy. The third peak corresponds to the activation and the migration of non interacting kinks, on segments containing weak obstacles, identified as boron atoms in doped specimens. The activation energy (2.4 eV) corresponds to the sum of the migration and nucleation energies.
As regards the low frequency background, it is attributed to the supplementary glide induced by kink absorption at triple nodes.

Résumé
La mobilité des dislocations dans le silicium monocristallin a été étudiée par frottement intérieur en balayage de fréquence. Trois pics de relaxation superposés à un fond de basse fréquence ont été observés sur des échantillons préalablement déformés.
Le premier pic a été attribué à la migration des décrochements géométriques avec une énergie W_M de 1,5 eV. Le second, d'énergie d'activation 1,95 eV, a été rattaché à la création et à l'interaction entre décrochements thermiques ; l'énergie de formation F_{DK} déduite est de 0,9 eV. Le troisième pic, d'énergie 2,4 eV a été associé au mouvement des décrochements thermiques dans un champ d'impuretés identifiés aux atomes de dopant.
Le fond de basse fréquence provient de l'absorption des décrochements aux noeuds du réseau.

Introduction

Due to the high Peierls potentials existing in covalent materials, double-kink formation relaxation is expected to occur at very high temperatures. Furthermore, recent investigations in plasticity /1,2,3/ have shown that the kink migration energy is much higher than predicted by previous internal friction measurements /4,5/ at low or medium temperatures.
However high temperature results /6,7,8/ in Ge did not reveal any intrinsic dislocation relaxation but an increase of the background damping with the temperature. The frequency range used in conventional internal friction tests does not permit

one to reach the high temperature range where relaxation is expected to occur.
In the present work, an apparatus allowing isothermal internal friction measurements at very low frequencies, fit for the study of high activation energy relaxation effects, was used.

Experimental conditions

FZ WAZO silicon single crystal with boron and phosphorus doping were used. Blocks ($20 \times 6 \times 6$ mm^3) were deformed by compression along the main axis. Due to the strain rate, the temperature and the crystal orientation, different microstructures were obtained.

Deformation	Doping at./cm^3	Compression axis	Strain % (stage)	Temperature (K)	Etch pit observation /9/
1	B 9.10^{16}	$[1\bar{1}0]$	0.4 (I)	1320	Dislocation bands $10^7 < \rho < 5.10^7$cm^{-2}
2	B 9.10^{16}	$[1\bar{1}0]$	1.4 (I)	1050	Homogeneous structure $\rho = 4.10^6$cm^{-2}
3	B 9.10^{16}	$[1\bar{1}0]$	1.2 (I)	1150 + 820	Dislocation bands $\rho = 3.10^7$ cm^{-2}
4	B 9.10^{16}	$[1\bar{1}0]$	indetermined "in situ"		Very inhomogeneous
5	P 10^{13}	$[2\bar{3}1]$	3.4 (II)	1220	Ineffective
6	P 6.10^{18}	$[2\bar{3}1]$	2.7 (II)	1220	$2 < \rho < 4.10^7$cm^{-2}
7	P 6.10^{18}	$[2\bar{3}1]$	4.0 (II)	1220	$2.10^7 < \rho < 10^8$cm^{-2}

TABLE 1

Internal friction specimens were cut from the prestrained blocks along the main axis. Specimens were then mechanically polished to remove surface dislocation sources.
The experimental internal friction arrangement allowing measurements in a wide frequency and temperature range, on brittle specimens, has been described elsewhere /10/. Tests were performed under vacuum : 5.10^{-6} Torr.

Experimental results

No dislocation relaxation effect was observed below 970 K, confirming that silicon plasticity is negligible below 0.6 Tm. A low frequency exponential background appears about 970 K corresponding to the high temperature background previously observed in Si /11/ and Ge /5,6,7/.

Additional relaxation effects are also observed in certain cases, depending on deformation and doping conditions.

a) Low frequency background analysis

Experimental spectra, similar to that shown in Fig.1, have been brought out according to the following steps :

a-1) Log $(Q^{-1} - Q_0^{-1})$ has been plotted versus log(ω) (Fig.2) (ω being the vibration angular frequency and Q_0^{-1} the background of the apparatus). When no relaxation peak occurs, the background is a straight line which can be accurately obtained :

$$\text{Log } Q_F^{-1} = \text{Log } A(T) - \alpha(T) \log(\omega)$$

a-2) The background corresponding to log $\omega = 0$, versus the inverse absolute temperature (Fig.3), is also linear :

$$\frac{\Delta \text{Log}(Q_F^{-1})}{\Delta(1/T)} = -\frac{H_A}{kT} \quad ; \; H_A \text{ being the apparent activation energy.}$$

a-3) From Fig.2 it is shown that :

$$\alpha(T) = \frac{\Delta(\log Q_F^{-1})}{\Delta(\log \omega)} = -\beta T + \gamma \; ; \; \beta \text{ and } \gamma \text{ constant parameters.}$$

These different steps lead to the final expression for the background :

$$Q_F^{-1} = A_0 e^{-H_A/kT} / \omega^{-\beta T + \gamma}$$

According to SCHOECK et al./12/, the true activation energy associated with the background is : $H_F = \frac{1}{\gamma} H_A$

The H_F, β and γ parameters are very sensitive to the microstructure of the specimens and are listed in Table II, for the different deformations.

Deformation	β ($10^{-3} K^{-1}$)	γ	H_F (eV)
1	0.86	1.54	1.54
2	0.26	0.53	1.74
3	0.26	0.54	1.86
5	0.70	1.11	1.93
6	0.49	0.86	1.90
7	0.34	0.77	1.86

TABLE II - Background parameters

b) Relaxation peaks

Relaxation peaks are obtained after removing the low frequency background. However these peaks are clearly defined only in prestrained specimens of p type.

In that case three well defined peaks could be analyzed, whose existence depends on the deformation conditions. The corresponding relaxation parameters are listed in table III.

Peak	Figure	Deformation	$H_{P_{eV}}$	τ_o (s)
P_1	Fig.4	1 2 4	2.36 2.39 2.38	1.3×10^{-10} 0.7×10^{-10} 0.8×10^{-10}
P_2	Fig.5	1	1.50	2.0×10^{-8}
P_3	Fig.6	3	1.95	1.2×10^{-8}

TABLE III - Relaxation parameters for P_1, P_2 and P_3 peaks

From these results, it is clear that P_1 peak is present in all specimens prestrained at temperatures beyond $0.6T_m$. The activation energy and the limit relaxation time are found insensitive to the dislocation microstructure.
P_3 peak appears only after the specimens have been strained at low temperature. Conversely P_2 peak is observed only after high temperature deformation. An increase of the relaxation strengths with temperature is also observed.

Discussion

These three peaks can be associated with three different dislocation glide mechanisms, assuming the following points :
-geometrical kinks are abrupt /13/ and the kink migration is thermally activated when : $W_M > kT$, W_M being the kink migration energy, the dislocation velocity given by $v_d = v_k C_k h$ with $\begin{cases} C_k : \text{kink density per unit length} \\ v_k : \text{kink velocity} \end{cases}$
- the glide of straight segments, parallel to the Peierls valleys, occurs through thermal double-kink nucleation and migration enhanced by the applied stress /14/.
Following the proposed model /13/, two cases must be distinguished :

$L < L_C \quad v_d = J h L$
$L > L_C \quad v_d = \sqrt{J v_k} h$

$\begin{cases} L : \text{segment length} \\ J : \text{nucleation rate} \\ L_C = 2X \text{ where } X \text{ is the simple kink mean free path} \\ h : \text{distance between Peierls valleys} \\ F_{DK} : \text{double-kink formation energy} \end{cases}$

In the case of a low amplitude applied stress, v_k could be determined by the Einstein relation:

$$v_k = \frac{\nu_D a^2 bh}{kT} e^{-W_M/kT} (\sigma - \epsilon/\delta J) \text{ ; where } \frac{\epsilon}{\delta J} V = \frac{abh}{2} \text{ is the restoring stress.}$$

P_2 peak can be associated with the relaxation of misoriented segments produced during the high temperature deformation.
The anelastic component is then expressed as :

$$\dot{\varepsilon} = \rho_2 b v_d = \rho_2 C_k \frac{a^2 b^2 h^2}{kT} \nu_D (\sigma - \varepsilon/\delta J) e^{-W_M/kT}$$

where ρ_2 is the effective density of active segments.
The activation energy can be identified as W_M = 1.5 eV.
P_1 and P_3 peaks associated with activation energies greater than W_M, arise from glide mechanisms involving double-kink nucleation on straight segments.
P_3 peak is correlated to impurity free segments developed during the low temperature deformation. In that case the kinks can interact, and the dislocation velocity is given by $v_d = \sqrt{J v_K}\, h = \frac{h}{a} e^{-F_{DK}/2kT} V_k$

In contrast, P_1 peak is observed when weak obstacles on the dislocation line inhibit single kink migration. They are identified as boron atoms, whose mean separation ℓ is less than L_c for the experimental conditions ($\ell \simeq 3.10^{-2}$ µm). An obstacle is overcome when it is reached by two successive kinks drifting from opposite directions . The whole dislocation velocity is then equal to the free segment component velocity : $v_d = J h \ell = (\ell/h) \exp(-F_{DK}/kT)\, v_k$.
These results are summarized in table IV.

	Energy	τ_o (prop.to)	Mechanism	Temperature
P_2	W_M	L^2	geometrical kinks	$T \simeq T_{ather}$
P_1	$W_M + F_{DK}$	$L^2 (h/\ell)(\ell<L_c)$	Thermal kinks-obstacles	$T > 0.6\ T_m$
P_3	$W_M + F_{DK}/2$	L^2	Interacting thermal kinks	$T < 0,6\ T_m$

TABLE IV

The background energy has been found between W_M and $W_M + F_{DK}/2$; we propose to connect it to the absorbtion of kinks at extended nodes, inducing a supplementary non reversible glide motion.

REFERENCES

/1/ - ALEXANDER, In Dislocations 84. P. Veyssière et al. édit., Editions CNRS Paris (1984) p. 283.
/2/ - FARBER, IUNIN, KIKITENKO, Phys. Stat. Sol. (a) 97 (1986) p. 469.
/3/ - LOUCHET, Inst. Phys. Conf. Serv. 60 (1981) p. 35.
/4/ - CALZECCHI, GONDI, MANTOVANI, Journal of Appl. Phys. 40 (12) (1969) p. 4798.
/5/ - OHORI, SUMINO, Phys. Stat. Sol. (a) 14 (1972) p. 489.
/6/ - GERK, WILLIAMS, J. Appl. Phys. 53(5) (1982) p. 3595.
/7/ - WELSCH, MITCHEL, GIBALA, Phys. Stat. Solid (a) 15 (1973) p. 225.

/8/ - MOLLER, JENDRICH, In Deformation of Ceramic Materials II 118, Plenum Press, New-York and London (1984) p. 25.

/9/ - SCHIMMEL, J. Electrochimical Society (1979) p. 479.

/10/- WOIRGARD, SARRAZIN, CHAUMET, Rev. Sci. Instrum. 48(10) (1977) 1322.

/11/- SOUTHGATE, MENDELSON, J. of Appl. Phys. 36(9) (1965) p. 2685.

/12/- SCHOECK, BISOGNI, SHYNE, Acta Met. 12 (1964) 1466.

/13/- BRAILSFORD, Phys. Rev. 122 (1961) p. 778.

/14/- HIRTH, LOTHE in Theory of Dislocations M.C. Graw-Hill, New-York, 1968.

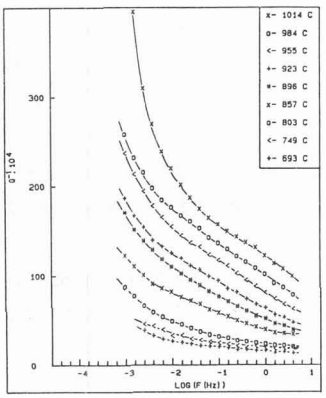

Fig.1- Damping curves Si p(B) 1.2 % strained at 1150 then 820 K.

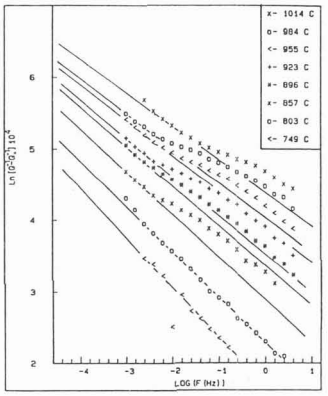

Fig.2 - Determination of the low frequency background from Fig.1.

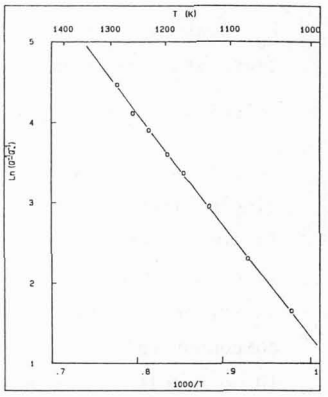

Fig.3 - Determination of A(T) for log (ω) = 0 (see text).

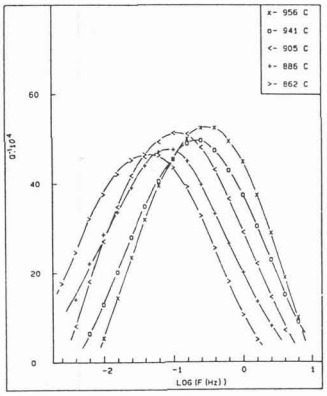

Fig.4 - Peak 1.

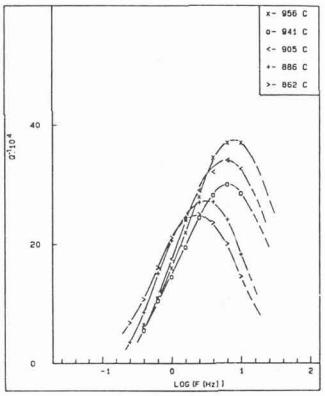

Fig.5 - Peak 2 Si p(B) 0.4 % strained at 1320 K.

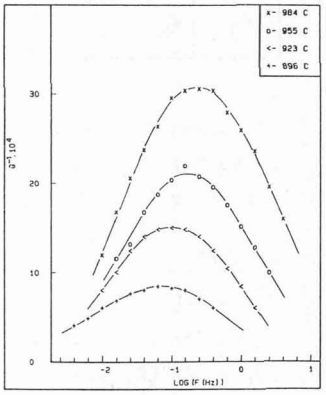

Fig. 6 - Peak 3 Si p(B) 1.2 % strained at 1150 then 820 K.